A Fractional Derivative Viscoelastic Model for Hybrid Active-Passive Damping Treatments in Time Domain - Application to Sandwich Beams

Ana Cristina Galucio, Jean-François Deü, Roger Ohayon

A Fractional Derivative Viscoelastic Model for Hybrid Active–Passive Damping Treatments in Time Domain – Application to Sandwich Beams

A. C. GALUCIO,* J.-F. DEÜ AND R. OHAYON

Structural Mechanics and Coupled Systems Laboratory, Conservatoire National des Arts et Métiers 2 rue Conté, 75003 Paris, France

ABSTRACT: This work presents a finite element formulation for the dynamic transient analysis of a damped adaptive sandwich beam composed of a viscoelastic core and elastic–piezoelectric laminated faces. The latter are modeled using the classical laminate theory, which takes the electromechanical coupling into account by modifying the stiffness of the piezoelectric layers. For the core, a fractional derivative model is used to characterize its viscoelastic behavior. Equations of motion are solved using a direct time integration method based on the Newmark scheme in conjunction with the Grünwald approximation of fractional derivatives. Emphasis is given to the finite element implementation of the fractional derivative model and to the influence of the electromechanical coupling.

Key Words: hybrid piezoelectric–viscoelastic damping treatment, fractional derivatives, sandwich beam, finite element method, transient dynamic analysis

INTRODUCTION

MANY investigations have demonstrated the potential of viscoelastic materials to improve the dynamics of lightly damped structures. There are numerous techniques to incorporate these materials into structures. Among them, the constrained layer passive damping treatment is already largely used to reduce structural vibrations, and more and more in conjunction with active vibration control (Baz, 1997; Trindade et al., 2001). The satisfactory performance of the passive treatments combined with the progress obtained in the field of the smart structures has motivated the development of hybrid active–passive damping treatments. This kind of technique consists of either adding to or replacing the elastic constraining layer by a piezoelectric one. In the context of hybrid damping treatments, classical dynamic formulations are usually employed while the viscoelastic models are relatively sophisticated. For example, adaptive composite-laminated plates with active constrained layer damping have been studied by Yi and Sze (2000) using a Prony series representation of the viscoelastic behavior. Lesieutre and Lee (1996) have used hybrid active–passive treatment with a time-domain viscoelastic model based on anelastic displacement fields (ADF). In the same context, Trindade et al. (2001) have used the Golla–Hughes–McTavish (GHM) mini-oscillator viscoelastic model (Golla and Hughes, 1985). All these damping models involve ordinary integer differential operators that are relatively easy to manipulate. The Prony series method is largely used in commercial finite element codes due to the low numerical cost introduced by the representation of the relaxation function in terms of decreasing exponentials. For the ADF and GHM approaches, additional damping coordinates are used to more accurately describe the frequency dependence of the viscoelastic material. Usually, the frequency band chosen for performing the curve fitting of master curves is the transition band since it is the region where the loss factor attains its maximum value. Furthermore, all these approaches can provide a state-space form of the structural equations in order to facilitate the implementation of a control law. However, due to the important number of material parameters needed, these curve fitting procedures can quickly become cumbersome. One of the alternatives to overcome this limitation is the utilization of fractional derivative rheological models.

In this work, a finite element formulation for transient dynamic analysis of sandwich beams with active constrained layer damping treatment is proposed. The sandwich beam is composed of a viscoelastic core, which is entirely covered by elastic faces that are provided

*Author to whom correspondence should be addressed.
E-mail: galucio@cnam.fr

with piezoelectric patches on their top and bottom surfaces. The model combines a classical three-layer sandwich theory for the face–core–face system (i.e., Euler-Bernoulli faces and Timoshenko core) and a piecewise linear electric potential for each piezoelectric sublayer. The laminated piezoelectric faces are modeled using the classical laminate theory which takes the electromechanical coupling into account by modifying the stiffness of the piezoelectric layers. Concerning the viscoelastic damping, its mathematical representation is carried out by a four-parameter fractional derivative model (Bagley and Torvik, 1983). This choice is related to the small number of parameters necessary to take into account the frequency dependence of the material over a broad range of frequency. Moreover, this model can be easily extended in order to take into account the influence of the temperature. Two main hypotheses about the viscoelastic behavior are considered throughout this investigation: isothermal conditions and frequency-independent Poisson's ratio. For the finite element implementation of the fractional derivative viscoelastic model, the basic idea is to use the Grünwald formalism for the fractional order derivative of the stress–strain relation in conjunction with a time discretization scheme based on the Newmark method (Schmidt and Gaul, 2001; Galucio et al., 2004). For this purpose, the time-dependent terms, arising from the viscoelastic constitutive law, are shifted to the right-hand member of the governing equation, modifying in this way the transient excitations. A recent investigation on the finite element implementation of fractional derivative operators in the modeling of viscoelastic damping has been carried out by Galucio et al. (2004) in the context of structural dynamics. Such a theoretical formulation is used here together with a multilayer adaptive beam theory, which is validated through a static and a free-vibration analysis. The static analysis consists of comparing the numerical results with the analytical ones obtained by Zhang and Sun (1996) for a cantilevered elastic beam with short-circuited piezoelectric electrodes. Eigenfrequencies of a simply supported elastic–piezoelectric laminated beam are compared to those obtained with an exact three-dimensional solution. This analytical solution is based on the mixed state-space approach developed by Benjeddou and Deü (2001) for transverse shear actuation of plates in statics. It is extended here for extension actuation in cylindrical bending in order to validate the present finite element model through a free-vibration analysis. Some numerical examples are considered. The influence of the Grünwald series truncation over the dynamic response of the sandwich beam is emphasized. Finally, an example using a sensor voltage feedback control scheme is presented in order to show the effectiveness of the proposed numerical implementation of hybrid active–passive treatments.

THEORETICAL FORMULATION

Consider a sandwich beam composed of a viscoelastic core and elastic–piezoelectric laminated faces. The first part of this section addresses the kinematical assumptions for the mechanical displacement field and the electrostatic hypotheses for the electric potential. In the second part, constitutive equations for the piezoelectric and viscoelastic materials are outlined. Finally, the variational formulation derived from the Hamilton's principle is presented.

Mechanical and Electrical Field Assumptions

The sandwich beam is modeled using Euler-Bernoulli assumptions for the faces and Timoshenko ones for the core. The elastic–piezoelectric faces are modeled using the classical laminated theory with linear electric potential through the thickness of each piezoelectric sublayer.

The mechanical displacement field within the ith layer can be written as

$$u_{xi}(x, z, t) = u_i(x, t) - (z - z_i)\theta_i(x, t) \tag{1a}$$

$$u_{zi}(x, z, t) = w(x, t) \tag{1b}$$

where the subscript $i = a, b, c$ stands for upper (composed of N_a sublayers), lower (composed of N_b sublayers) and middle layers, respectively. u_{xi} and u_{zi} are the axial and transverse displacements of each layer, u_i and θ_i are the axial displacement of the center line and the fiber rotation of each layer, and w is the transverse displacement (see Figure 1).

Let us introduce the mean and relative axial displacements given by $\bar{u} = (u_a + u_b)/2$ and $\tilde{u} = u_a - u_b$. Euler-Bernoulli hypotheses for the faces lead to $\theta_k = w'$ for $k = a, b$ with $(\cdot)' = \partial(\cdot)/\partial x$. As all layers are supposed to be perfectly bonded, the displacement continuity conditions at the interface layers can be written as $u_{xa} = u_{xc}$ at $z = h_c/2$ and $u_{xb} = u_{xc}$ at $z = -h_c/2$. Therefore, axial displacements of the centerlines and rotations of each layer can be written in terms of w' and the above-defined variables $\bar{u}$ and $\tilde{u}$ as

$$\begin{gathered} u_a = \bar{u} + \frac{\tilde{u}}{2}, \quad \theta_a = w'; \qquad u_b = \bar{u} - \frac{\tilde{u}}{2}, \quad \theta_b = w'; \\ u_c = \bar{u} + \frac{\tilde{h}}{4} w', \quad \theta_c = -\frac{\tilde{u} + \bar{h} w'}{h_c} \end{gathered} \tag{2}$$

where $\bar{h}$ and $\tilde{h}$ are defined by $\bar{h} = (h_a + h_b)/2$ and $\tilde{h} = h_a - h_b$.

From (1) and (2), and taking the hypothesis of plane stress state into account, the axial strain of the ith layer ε_{1i} and the shear strain of the core ε_{5c} can be written

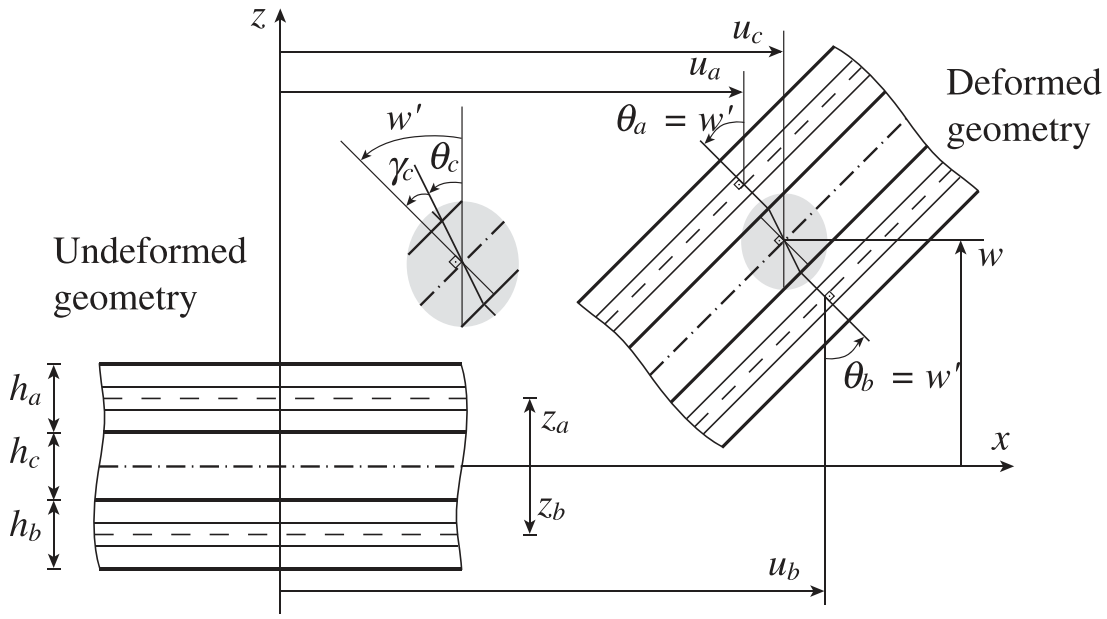

Figure 1. *Sandwich beam kinematics.*

as follows

$$\varepsilon_{1i} = \epsilon_i + (z - z_i)\kappa_i, \quad \varepsilon_{5c} = \gamma_c \tag{3}$$

where membrane strain ϵ_i and curvature κ_i of the ith layer, and shear strain of the core γ_c, are defined by

$$\epsilon_a = \bar{u}' + \frac{\tilde{u}'}{2}, \quad \epsilon_b = \bar{u}' - \frac{\tilde{u}'}{2}, \quad \kappa_a = \kappa_b = -w'' \tag{4}$$

$$\epsilon_c = \bar{u}' + \frac{\tilde{h}}{4}w'', \quad \kappa_c = \frac{\tilde{u}' + \bar{h}w''}{h_c}, \quad \gamma_c = \frac{\tilde{u}}{h_c} + \left(1 + \frac{\bar{h}}{h_c}\right)w' \tag{5}$$

Without covering face layers (i.e., $h_a = h_b = 0$), the previous generalized strain quantities of the core correspond to those of a single Timoshenko beam.

Concerning the electrostatic aspects, two main assumptions are taken under consideration. The first one concerns the electric potential, which is supposed to be linear within the thickness of each piezoelectric sublayer:

$$\phi_{k_j}(x, z, t) = \bar{\phi}_{k_j}(x, t) + (z - z_{k_j})\frac{V_{k_j}(x, t)}{h_{k_j}} \tag{6}$$

where $\bar{\phi}_{k_j} = (\phi^+_{k_j} + \phi^-_{k_j})/2$ and $V_{k_j} = \phi^+_{k_j} - \phi^-_{k_j}$. The quantities $\phi^+_{k_j}$ and $\phi^-_{k_j}$ are the electrical boundary conditions at the top $(z = z_{k_j} + h_{k_j}/2)$ and at the bottom $(z = z_{k_j} - h_{k_j}/2)$ surfaces. The local z-axis of the k_jth face sublayer is situated at (for $k = a(+),\ b(-)$)

$$z_{k_j} = \pm\frac{h_{k_j} + h_c}{2} \pm \sum_{r=1}^{j-1} h_{k_r}$$

with h_{k_j} being the thickness of the k_jth layer.

Second, the axial component of the electrical field can be neglected because its contribution to the electromechanical energy is small when compared to that of the transverse one (Trindade et al., 2001).

The two above assumptions imply a constant transverse electrical field within the k_jth piezoelectric sublayer:

$$E_{3k_j} = -\frac{\partial\phi_{k_j}}{\partial z} = -\frac{V_{k_j}}{h_{k_j}} \tag{7}$$

Piezoelectric Constitutive Equations

The piezoelectric sublayers of the laminated faces are poled in the thickness direction with an electrical field applied parallel to this polarization. Such a configuration is characterized by the electromechanical coupling between the axial strain ε_1 and the transverse electrical field E_3. The three-dimensional constitutive equations can be reduced to

$$\begin{aligned} \sigma_1 &= \bar{c}_{11}\varepsilon_1 - \bar{e}_{31}E_3 \\ D_3 &= \bar{e}_{31}\varepsilon_1 + \bar{d}_{33}E_3 \end{aligned} \tag{8}$$

where σ_1 and D_3 are the axial stress and the transverse electrical displacement. Modified elastic, piezoelectric and dielectric constants are respectively given by

$$\bar{c}_{11} = c_{11} - \frac{{c_{13}}^2}{c_{33}}, \quad \bar{e}_{31} = e_{31} - \frac{c_{13}e_{33}}{c_{33}}, \quad \bar{d}_{33} = d_{33} + \frac{{e_{33}}^2}{c_{33}} \tag{9}$$

For elastic faces, the piezoelectric constants vanish. Moreover, if the material is isotropic $\bar{c}_{11} = E/(1 - \nu^2)$,

where E and ν are the elastic modulus and the Poisson's ratio.

Viscoelastic Constitutive Equations

The one-dimensional constitutive equation introduced by Bagley and Torvik (1983) is adopted in this work to describe the viscoelastic behavior of the core:

$$\sigma_i + \tau^\alpha D^\alpha \sigma_i = \xi_i \left(\varepsilon_i + \tau^\alpha \frac{E_\infty}{E_o} D^\alpha \varepsilon_i \right) \tag{10}$$

where σ and ε are stress and strain. As the core behaves as a Timoshenko beam, let the subscript i stand for axial ($i=1$) and shear ($i=5$) components that are associated with the constants $\xi_1 = E_o/(1-\nu^2)$ and $\xi_5 = E_o/2(1+\nu)$. Furthermore, E_o and E_∞ are the relaxed and nonrelaxed elastic moduli, τ is the relaxation time, α is the fractional order of the time derivative ($0<\alpha<1$), and D^α denotes the operator of fractional derivation of αth order according to Riemann-Liouville definition

$$D^\alpha \sigma(t) = \frac{1}{\Gamma(1-\alpha)} \frac{d}{dt} \int_0^t \frac{\sigma(s)}{(t-s)^\alpha} \, ds$$

in which Γ is the gamma function.

This four-parameter fractional derivative model has been shown to be an effective tool to describe the weak frequency dependence of most viscoelastic materials (Bagley and Torvik, 1983; Pritz, 1996). Its behavior in the frequency domain is described between two asymptotic values: the static modulus of elasticity $E_o = E^*(\omega \to 0)$ and the high-frequency limit value of the dynamic modulus $E_\infty = E^*(\omega \to \infty)$, where $E^*(\omega)$ is the complex modulus of elasticity, which is obtained by the Fourier transform of Equation (10). The statements $0 < \alpha < 1$, $\tau > 0$, and $E_\infty > E_o$ fulfill the second law of thermodynamics.

The identification of the model parameters for the ISD112 at 27°C viscoelastic material is performed using the shear relaxed and nonrelaxed moduli (Galucio et al., 2004) that are proportional to the elastic ones since the Poisson's ratio is supposed to be frequency independent.

Variational Formulation

The dynamic equations of the previously described sandwich beam are derived from the Hamilton's principle

$$\int_{t_1}^{t_2} \left(\delta T - \delta U + \delta W \right) dt = 0 \tag{11}$$

where $\delta T = \delta T_a + \delta T_b + \delta T_c$ is the variation of the kinetic energy, $\delta U = \delta U_a + \delta U_b + \delta U_c$ is the variation of the internal energy, and δW is the variation of the work done by external forces acting on the system.

Using Equation (1), integrating by parts Equation (11), the variation of the kinetic energy of the kth lamina is written as (for $k = a, b$)

$$\begin{aligned} \delta T_k &= -\sum_{j=1}^{N_k} \int_{\Omega_{k_j}} \rho_{k_j} \left(\ddot{u}_{xk} \delta u_{xk} + \ddot{u}_{zk} \delta u_{zk} \right) d\Omega \\ &= -b \int_0^L \Big[I_0^k (\ddot{u}_k \delta u_k + \ddot{w} \delta w) \\ &\qquad - I_1^k (\ddot{u}_k \delta \theta_k + \ddot{\theta}_k \delta u_k) + I_2^k \ddot{\theta}_k \delta \theta_k \Big] dx \end{aligned} \tag{12}$$

where an over dot represents the differentiation with respect to time, b and L are the width and the length of the beam, and ρ_{k_j} and Ω_{k_j} are the mass density and the domain of the k_jth sublayer. The zero-, first-, and second-order inertia moments are classically defined as

$$\left[I_0^k, I_1^k, I_2^k \right] = \sum_{j=1}^{N_k} \rho_{k_j} \left[H_0^{k_j}, H_1^{k_j}, H_2^{k_j} \right]$$

where $H_0^{k_j}$, $H_1^{k_j}$, and $H_2^{k_j}$ are the thickness, the first and second moments of area by unit of width of each sublayer, respectively, defined by

$$\left[H_0^{k_j}, H_1^{k_j}, H_2^{k_j} \right] = \int_{z_{k_j} - h_{k_j}/2}^{z_{k_j} + h_{k_j}/2} \left[1, (z - z_k), (z - z_k)^2 \right] dz$$

The local z-axis of the kth face layer is situated at (for $k = a(+), b(-)$)

$$z_k = \pm \frac{1}{2} \left(h_c + \sum_{j=1}^{N_k} h_{k_j} \right)$$

The procedure used to compute the kinetic energy of the core is similar to the one for the faces. Then, the variation of the kinetic energy of the core is classically written as

$$\begin{aligned} \delta T_c &= -\int_{\Omega_c} \rho_c \left(\ddot{u}_{xc} \delta u_{xc} + \ddot{u}_{zc} \delta u_{zc} \right) d\Omega \\ &= -b \int_0^L \rho_c \left[h_c (\ddot{u}_c \delta u_c + \ddot{w} \delta w) + \frac{h_c^3}{12} \ddot{\theta}_c \delta \theta_c \right] dx \end{aligned} \tag{13}$$

where ρ_c and Ω_c are the mass density and the domain of the core.

As described above, the second term in the variational equation (11) corresponds to the virtual internal energy of the sandwich beam. Its electromechanical contribution associated with the kth lamina can be

written as

$$\begin{aligned}\delta U_k &= \sum_{j=1}^{N_k} \int_{\Omega_{k_j}} \left(\sigma_{1k_j}\delta\varepsilon_{1k} - D_{3k_j}\delta E_{3k_j}\right) d\Omega \\ &= \delta U_k^M + \delta U_k^{ME} + \delta U_k^{EM} + \delta U_k^E\end{aligned} \tag{14}$$

where δU_k^M and δU_k^E are the virtual mechanical and dielectrical internal energies, and δU_k^{ME} and δU_k^{EM} comprise the virtual piezoelectric internal energy, i.e., the electromechanical coupling.

Using strain relations (3), piezoelectric constitutive equations (8), and electrical field expression (7), each term in the right-hand side of Equation (14) is thoroughly described below. The virtual mechanical internal energy can be written as

$$\delta U_k^M = b\int_0^L \left[A^k\epsilon_k\delta\epsilon_k + B^k(\kappa_k\delta\epsilon_k + \epsilon_k\delta\kappa_k) + D^k\kappa_k\delta\kappa_k\right] dx \tag{15}$$

where A^k is the extensional stiffness, D^k is the bending stiffness, and B^k is the bending–extensional coupling stiffness defined as

$$\left[A^k,\ B^k,\ D^k\right] = \sum_{j=1}^{N_k} \bar{c}_{11}^{k_j}\left[H_0^{k_j},\ H_1^{k_j},\ H_2^{k_j}\right] \tag{16}$$

The three last terms in Equation (14) are related to the electromechanical coupling and the dielectrical quantities in the virtual internal energy of the faces. These terms are defined as follows

$$\delta U_k^{ME} = b\sum_{j=1}^{N_k}\int_0^L \bar{e}_{31}^{k_j} V_{k_j}\left[\delta\epsilon_k + (z_{k_j} - z_k)\delta\kappa_k\right] dx \tag{17a}$$

$$\delta U_k^{EM} = b\sum_{j=1}^{N_k}\int_0^L \bar{e}_{31}^{k_j}\left[\epsilon_k + (z_{k_j} - z_k)\kappa_k\right]\delta V_{k_j} dx \tag{17b}$$

$$\delta U_k^E = -b\sum_{j=1}^{N_k}\int_0^L \bar{d}_{33}^{k_j}\frac{V_{k_j}}{h_{k_j}}\delta V_{k_j} dx \tag{17c}$$

It is easy to see in Equations (17a) and (17b) that the electromechanical coupling is taken into account by means of the piezoelectric constant $\bar{e}_{31}^{k_j}$. This electromechanical coupling describes the so-called inverse and direct piezoelectric effects.

INVERSE PIEZOELECTRIC EFFECT (ACTUATOR)

An actuator configuration consists of applying an electric field to a piezoelectric ceramic in order to induce a mechanical deformation. This electric field is imposed by means of an external force, which is written as a function of the voltage applied to the piezoelectric patch. In this case, the variation of the difference of electrical potential of the k_jth lamina vanishes. This implies that the electromechanical coupling is described by Equation (17a). Consequently, the above-mentioned external force is extracted from Equation (17a) and is written in its discretized form later.

DIRECT PIEZOELECTRIC EFFECT (SENSOR)

The case where an electric field is induced by a mechanical deformation in the piezoelectric material corresponds to a sensor configuration. The unknown is the difference of electric potential of the k_jth piezoelectric layer. In this way, Equations (17b) and (17c) supply the following expression

$$E_{3k_j} = -\frac{\bar{e}_{31}^{k_j}}{\bar{d}_{33}^{k_j}}\left[\epsilon_k + (z_{k_j} - z_k)\kappa_k\right] \tag{18}$$

Substituting Equations (7) and (18) into (17a) and adding the result to (15), the virtual electromechanical internal energy of the kth lamina is rewritten as

$$\begin{aligned}\delta U_k = \delta U_k^m + b\int_0^L \Big[&\hat{A}^k\epsilon_k\delta\epsilon_k + \hat{B}^k(\kappa_k\delta\epsilon_k + \epsilon_k\delta\kappa_k) \\ &+ \hat{D}^k\kappa_k\delta\kappa_k\Big] dx\end{aligned} \tag{19}$$

where the terms related to the electromechanical coupling are given by

$$\left[\hat{A}^k, \hat{B}^k, \hat{D}^k\right] = \sum_{j=1}^{N_k}\frac{(\bar{e}_{31}^{k_j})^2}{\bar{d}_{33}^{k_j}}\left[H_0^{k_j}, H_1^{k_j}, (H_1^{k_j})^2/H_0^{k_j}\right] \tag{20}$$

In Equation (19), an increase in the stiffness of the beam due to the direct piezoelectric effect is noted.

For the sake of simplicity, the core is assumed to be elastic (i.e., $\tau = 0$) in this section. Then, the virtual internal energy of the core is given by

$$\begin{aligned}\delta U_c &= \int_{\Omega_c}\left(\sigma_{1c}\delta\varepsilon_{1c} + \sigma_{5c}\delta\varepsilon_{5c}\right) dV \\ &= b\int_0^L\left[\frac{E_o}{1-\nu^2}\left(h_c\epsilon_c\delta\epsilon_c + \frac{h_c^3}{12}\kappa_c\delta\kappa_c\right) + \frac{E_o}{2(1+\nu)}h_c\gamma_c\delta\gamma_c\right] dx\end{aligned} \tag{21}$$

The viscoelastic behavior of the core will be addressed in the following section.

FINITE ELEMENT MODEL

The finite element formulation of the three-layer sandwich beam is thoroughly described in (Galucio et al., 2004). Such a formulation is extended here to the case of a beam composed of elastic–piezoelectric laminated faces and a viscoelastic core. We recall

that the displacements are discretized with linear (axial displacement) and cubic (deflection) shape functions. They are related to the elementary degrees-of-freedom vector $\mathbf{q}_e = [\bar{u}_1\ w_1\ w_1'\ \tilde{u}_1 | \bar{u}_2\ w_2\ w_2'\ \tilde{u}_2]$ by

$$u_i = \mathbf{H}_{xi}\mathbf{q}_e, \quad w = \mathbf{H}_z\mathbf{q}_e, \quad \theta_i = \mathbf{H}_{ri}\mathbf{q}_e \tag{22}$$

where $i = a,\ b,\ c$ and where the subscripts x, z, and r stand for axial displacement, transverse displacement, and rotation. Let subscript e stand for elementary quantities. Moreover, membrane, bending, and shear strains can be expressed by

$$\epsilon_i = \mathbf{B}_{mi}\mathbf{q}_e, \quad \kappa_i = \mathbf{B}_{bi}\mathbf{q}_e, \quad \gamma_c = \mathbf{B}_{sc}\mathbf{q}_e \tag{23}$$

Using Equations (22) and (23), the discretization of the variation of the kinetic energy, the virtual internal energy and the work done by external forces is $\delta T_e = -\delta\mathbf{q}_e^T\mathbf{M}_e\ddot{\mathbf{q}}_e$, $\delta U_e = \delta\mathbf{q}_e^T\mathbf{K}_e^*\mathbf{q}_e$, and $\delta W_e = \delta\mathbf{q}_e^T\mathbf{F}_e^*$. Consequently, the equation of motion of the system is written as

$$\mathbf{M}_e\ddot{\mathbf{q}}_e^{n+1} + \mathbf{K}_e^*\mathbf{q}_e^{n+1} = \mathbf{F}_e^{*n+1} \tag{24}$$

where $\mathbf{M}_e$ is the mass matrix of the beam defined by $\mathbf{M}_e = \mathbf{M}_e^a + \mathbf{M}_e^b + \mathbf{M}_e^c$. The stiffness matrix of the beam $\mathbf{K}_e^*$ and the external force vector $\mathbf{F}_e^*$ comprise the piezoelectric behavior of the laminated faces and the viscoelastic behavior of the core. In the following, these terms will be first described for the piezoelectric faces (assuming an elastic core) and then for the viscoelastic core (assuming elastic faces). Finally, a complete formulation which takes piezoelectric and viscoelastic aspects into account is presented.

Piezoelectric Laminated Faces

The finite element formulation used to describe the coupling between the electrical and mechanical properties of a laminated beam has no electrical degrees of freedom. The electromechanical coupling is made by changing the stiffness of the piezoelectric layer (sensor configuration) or by modifying an electric field within the piezoelectric layer (actuator configuration). Since the electric potential is supposed to be linear through the thickness of the piezoelectric ceramic, the electromechanical coupling is neglected for a short-circuited piezoelectric layer. This formulation requires a post-treatment of results in order to obtain the induced voltage within the piezoelectric patches taken as sensors.

In the following, mass and stiffness matrices of the piezoelectric faces are written in terms of membrane, bending, and a membrane–bending coupling term.

The element mass matrix of each piezoelectric face ($k = a,\ b$), arising from the discretization of Equation (12), is given by

$$\mathbf{M}_e^k = b\int_0^{L_e}\left[I_0^k\left(\mathbf{H}_{xk}^T\mathbf{H}_{xk} + \mathbf{H}_z^T\mathbf{H}_z\right) - I_1^k\left(\mathbf{H}_{xk}^T\mathbf{H}_{rk} + \mathbf{H}_{rk}^T\mathbf{H}_{xk}\right) + I_2^k\mathbf{H}_{rk}^T\mathbf{H}_{rk}\right]dx \tag{25}$$

After discretizing Equation (15), the elementary mechanical stiffness matrix of each piezoelectric face ($k = a, b$) is defined as

$$\mathbf{K}_e^k = b\int_0^{L_e}\left[A^k\mathbf{B}_{mk}^T\mathbf{B}_{mk} + B^k(\mathbf{B}_{mk}^T\mathbf{B}_{bk} + \mathbf{B}_{bk}^T\mathbf{B}_{mk}) + D^k\mathbf{B}_{bk}^T\mathbf{B}_{bk}\right]dx \tag{26}$$

If the laminate is constructed such that it has complete symmetry of individual lamina thickness, properties, and orientations about the middle plane of the laminate, then there is no coupling between bending and membrane effects ($B^k = 0$). For an orthotropic material, the constants $\bar{c}_{11}^{k_j}$ can be simply written as functions of the elastic components as in Equation (9).

INVERSE PIEZOELECTRIC EFFECT (ACTUATOR)

If an electric field is imposed through the thickness of the piezoelectric patches, the equation of motion of the structure, whose core is supposed to be elastic, is given by

$$\mathbf{M}_e\ddot{\mathbf{q}}_e^{n+1} + \mathbf{K}_e\mathbf{q}_e^{n+1} = \hat{\mathbf{F}}_{ek_j}^{n+1} \tag{27}$$

where the elementary stiffness matrix is $\mathbf{K}_e = \mathbf{K}_e^a + \mathbf{K}_e^b + \mathbf{K}_e^c$. The applied electrical field corresponds to an electrical force which arises from the discretization of Equation (17a):

$$\hat{\mathbf{F}}_{ek_j}^{n+1} = -b\int_0^{L_e}\bar{e}_{31}^{k_j}V_{k_j}^{n+1}\left[\mathbf{B}_{mk}^T + (z_{k_j} - z_k)\mathbf{B}_{bk}^T\right]dx \tag{28}$$

It is noted that the electromechanical coupling is taken into account by means of this external force.

DIRECT PIEZOELECTRIC EFFECT (SENSOR)

For a sensor configuration, the stiffness matrix is modified in order to take the electromechanical coupling into account according to Equations (17b) and (17c), since the electrical field is unknown. The equation of motion of the structure with an elastic core is then written as

$$\mathbf{M}_e\ddot{\mathbf{q}}_e^{n+1} + (\mathbf{K}_e + \hat{\mathbf{K}}_e)\mathbf{q}_e^{n+1} = \mathbf{F}_e^{n+1} \tag{29}$$

where $\mathbf{F}^{n+1}$ is the external force vector and $\hat{\mathbf{K}}_e = \hat{\mathbf{K}}_e^a + \hat{\mathbf{K}}_e^b$ is the supplementary stiffness matrix arising

from the discretization of Equation (19), given by (for $k = a,\ b$)

$$\hat{\mathbf{K}}_e^k = b\int_0^{L_e}\Big[\hat{A}^k\mathbf{B}_{mk}^T\mathbf{B}_{mk} + \hat{B}^k(\mathbf{B}_{mk}^T\mathbf{B}_{bk} + \mathbf{B}_{bk}^T\mathbf{B}_{mk}) + \hat{D}^k\mathbf{B}_{bk}^T\mathbf{B}_{bk}\Big]dx \tag{30}$$

After solving Equation (29), the electrical field in the k_j piezoelectric sublayer is simply obtained using Equation (18). This method of posttreating the results in order to obtain the difference of electric potential is equivalent to the one used by Trindade et al. (2001), which consists of introducing electrical degrees of freedom in the finite element formulation and then to carry out a static condensation *a posteriori*.

Viscoelastic Core

The equation of motion of the beam, assuming elastic laminated faces and viscoelastic core, is given by

$$\mathbf{M}_e\ddot{\mathbf{q}}_e^{n+1} + (\mathbf{K}_e^a + \mathbf{K}_e^b)\mathbf{q}_e^{n+1} + \int_{\Omega_e^c}\mathbf{B}_c^T\sigma_c^{n+1}d\Omega = \mathbf{F}_e^{n+1} \tag{31}$$

where $\mathbf{K}^k$ ($k = a,\ b$) is the mechanical stiffness matrix of the faces (Equation (26)) and the mass matrix of the core is classically defined as

$$\mathbf{M}_e^c = b\int_0^{L_e}\rho_c\left[h_c\left(\mathbf{H}_{xc}^T\mathbf{H}_{xc} + \mathbf{H}_z^T\mathbf{H}_z\right) + \frac{h_c^3}{12}\mathbf{H}_{rc}^T\mathbf{H}_{rc}\right]dx \tag{32}$$

where ρ_c is the mass density of the core.

Concerning the stiffness matrix of the core, the third term on the left-hand side of Equation (31) can be developed as

$$\int_{\Omega_e^c}\mathbf{B}_c^T\sigma_c^{n+1}d\Omega = \int_{\Omega_e^c}\left[(\mathbf{B}_{mc}^T + z\mathbf{B}_{bc}^T)\sigma_{1c}^{n+1} + \mathbf{B}_{sc}^T\sigma_{5c}^{n+1}\right]d\Omega \tag{33}$$

If the core is elastic, i.e. $\sigma_{1c} = \xi_1\varepsilon_{1c}$ and $\sigma_{5c} = \xi_5\varepsilon_{5c}$, this last expression corresponds to $\mathbf{K}_e^c\mathbf{q}_e^{n+1}$, with

$$\mathbf{K}_e^c = b\int_0^{L_e}\left[\frac{E_o}{1-\nu^2}\left(h_c\mathbf{B}_{mc}^T\mathbf{B}_{mc} + \frac{h_c^3}{12}\mathbf{B}_{bc}^T\mathbf{B}_{bc}\right) + \frac{E_o}{2(1+\nu)}h_c\mathbf{B}_{sc}^T\mathbf{B}_{sc}\right]dx \tag{34}$$

APPROXIMATION FOR FRACTIONAL DERIVATIVES

The fractional operator D^α, appearing in the constitutive equation (10), can be approximated by several methods. One of them is the Grünwald definition, which is often adopted in literature as it is valid for all values of α and easy to implement numerically. The finite difference approximation of the Grünwald definition is given by

$$(D^\alpha f)_n \approx \frac{1}{\Delta t^\alpha}\sum_{j=0}^{N_t}A_{j+1}f_{n-j} \tag{35}$$

where Δt is the time step increment of the numerical scheme (the function f_n is approximated by $f(t_n)$, with $t_n = n\Delta t$), N_t is the truncation number of the series, and A_{j+1} represents the Grünwald coefficients given either in terms of the gamma function or by a recurrence formula

$$A_{j+1} = \frac{\Gamma(j-\alpha)}{\Gamma(-\alpha)\Gamma(j+1)} \qquad \text{or} \qquad A_{j+1} = \frac{j-\alpha-1}{j}A_j$$

Let us introduce the internal variable as a strain function $\bar{\varepsilon}_i = \varepsilon_i - E_o\sigma_i/(\xi_i E_\infty)$, such that the constitutive equation (10) can be rewritten as (Galucio et al., 2004)

$$\bar{\varepsilon}_i + \tau^\alpha D^\alpha\bar{\varepsilon}_i = \frac{E_\infty - E_o}{E_\infty}\varepsilon_i \tag{36}$$

This variable change implies that Equation (36) contains only one fractional derivative term instead of two as in (10). Using the Grünwald approximation (35) and noting that $A_1 = 1$, relation (36) takes the following discretized form

$$\bar{\varepsilon}_i^{n+1} = (1-c)\frac{E_\infty - E_o}{E_\infty}\varepsilon_i^{n+1} - c\sum_{j=1}^{N_t}A_{j+1}\bar{\varepsilon}_i^{n+1-j} \tag{37}$$

where c is a dimensionless constant given by $c = \tau^\alpha/(\tau^\alpha + \Delta t^\alpha)$.

It should be stated that the Grünwald coefficients in Equation (37), which are strictly decreasing when j increases, describe the fading memory phenomena. In other words, the behavior of the viscoelastic material at a given time step depends more strongly on the recent time history than on the distant one.

Combining the variable change described above with Equation (37) and substituting the result into (33), one obtains

$$\int_{\Omega_e^c}\mathbf{B}_c^T\sigma_c^{n+1}d\Omega = \left(1 + c\frac{E_\infty - E_o}{E_o}\right)\mathbf{K}_e^c\mathbf{q}_e^{n+1} + c\int_{\Omega_e^c}\Big[(\mathbf{B}_{mc}^T + z\mathbf{B}_{bc}^T)\sum_{j=1}^{N_t}A_{j+1}\bar{\boldsymbol{\sigma}}_{1c}^{n+1-j} + \mathbf{B}_{sc}^T\sum_{j=1}^{N_t}A_{j+1}\bar{\boldsymbol{\sigma}}_{5c}^{n+1-j}\Big]d\Omega \tag{38}$$

so that the elementary semidiscrete equation of motion (31) can be rewritten as follows

$$\mathbf{M}_e\ddot{\mathbf{q}}_e^{n+1} + (\mathbf{K}_e + \bar{\mathbf{K}}_e)\mathbf{q}_e^{n+1} = \mathbf{F}_e^{n+1} + \bar{\mathbf{F}}_e^{n+1} \tag{39}$$

where the modified stiffness matrix $\bar{\mathbf{K}}_e$ and loading vector $\bar{\mathbf{F}}_e^{n+1}$, arising from the viscoelastic behavior of the core, are given by

$$\bar{\mathbf{K}}_e = c\frac{E_\infty - E_o}{E_o}\mathbf{K}_e^c \tag{40}$$

$$\bar{\mathbf{F}}_e^{n+1} = -c\frac{E_\infty}{E_o}\mathbf{K}_e^c\sum_{j=1}^{N_t} A_{j+1}\bar{\mathbf{q}}_e^{n+1-j} \tag{41}$$

By abuse of language, we shall denote the discretized unknowns $\bar{\mathbf{q}}_e^{n+1}$, associated with $\bar{\varepsilon}$, by ''anelastic displacements''. These unknowns depend on the displacement memory and are updated using the following equation

$$\bar{\mathbf{q}}_e^{n+1} = (1-c)\frac{E_\infty - E_o}{E_\infty}\mathbf{q}_e^{n+1} - c\sum_{j=1}^{N_t} A_{j+1}\bar{\mathbf{q}}_e^{n+1-j} \tag{42}$$

It should be noted that the vector $\bar{\mathbf{q}}$ does not constitute a new degree of freedom in the system, it is just a numerical artifice used in the time integration scheme for the characterization of the fading memory phenomena.

General Case

Finally, the equation of motion (24) can be rewritten for a complete configuration with piezoelectric faces (sensor–actuator) and a viscoelastic core:

$$\mathbf{M}_e\ddot{\mathbf{q}}_e^{n+1} + (\mathbf{K}_e + \hat{\mathbf{K}}_e + \bar{\mathbf{K}}_e)\mathbf{q}_e^{n+1} = \mathbf{F}_e^{n+1} + \hat{\mathbf{F}}_{ek_j}^{n+1} + \bar{\mathbf{F}}_e^{n+1} \tag{43}$$

where the mass matrix $\mathbf{M}_e$ arises from the sum of Equations (25) and (32), while the stiffness matrix $\mathbf{K}_e^*$ is split up into three terms: (i) $\mathbf{K}_e$ associated with an elastic behavior of faces-core which is composed of the sum of the Equations (26) and (34); (ii) $\hat{\mathbf{K}}_e$ associated with a sensor configuration of the faces (Equation (30)); and (iii) $\bar{\mathbf{K}}_e$ associated with the viscoelastic behavior of the core (Equation (40)). Concerning the right-hand side of Equation (43), $\mathbf{F}_e^*$ is composed of a mechanical external load $\mathbf{F}_e$, an electrical force $\hat{\mathbf{F}}_e$ associated with the actuator configuration for the faces (Equation (28)), and a dissipative force $\bar{\mathbf{F}}_e$ associated with the viscoelastic behavior of the core (Equation (41)). It is worthwhile to notice that all the time history-dependent terms were shifted to the right-hand side of the governing equation.

ALGORITHM IMPLEMENTATION

The Newmark scheme is adopted here due to its versatility for implementation in structural dynamics. Some modifications are carried out in the classical algorithm in order to obtain a modified scheme that is suitable to achieve the transient responses of a sandwich beam with laminated elastic–piezoelectric faces and a viscoelastic core in fractional calculus. The Newmark parameters $\beta = 1/4$ and $\gamma = 1/2$ are chosen in order to obtain an unconditionally stable and second-order accurate scheme. From Equation (41), it is noted that this approach requires the storage of the ''anelastic displacement'' history (Galucio et al., 2004). Concerning the stiffness matrix evaluation, recall that for a constant time step, it is evaluated once.

VALIDATION ASPECTS

The first part of this section focuses on the validation of the finite element formulation of the multilayer beam based on the comparison with the analytical results found in literature. Two analyses have been chosen for this: a static and a free-vibration analysis with different mechanical and electrical boundary conditions. Concerning the viscoelastic behavior of the core, some examples of validation were carried out in a previous work (Galucio et al., 2004).

The first example is extracted from the work of Zhang and Sun (1996). Consider a clamped-free sandwich beam composed of an elastic core (aluminum) entirely covered by piezoelectric faces (PZT5H). The latter are short-circuited and the voltage applied to each of the piezoelectric actuators is 20 V. The mechanical and piezoelectric properties of the beam are described in Table 1. The geometrical characteristics are: length – 100 mm, thickness of the elastic core – 16 mm, and thickness of each piezoelectric layer – 1 mm. In Figure 2(a), the typical quadratic behavior of the tip deflection when the beam is actuated by extension is noted. It is observed that the finite element result (with 10 elements) is in very good agreement with the analytical solution. The variation of the axial stress is shown in Figure 2(b), where one can observe very clearly the discontinuity at the layer interfaces. Horizontal solid lines indicate the geometrical position of each sublayer in the sandwich beam.

The second example of validation consists of a simply supported five-layer beam composed of a soft elastic core ($E = 1.5$ MPa, $\nu = 0.5$, and $\rho = 1600\,\mathrm{kg/m^3}$) covered by symmetrical elastic layers (aluminum) that are

Table 1. Mechanical and piezoelectric characteristics of the sandwich beam.

Aluminum	$\rho = 2690\,\mathrm{kg/m^3}$, $\nu = 0.345$, $E = 70.3$ GPa
PZT5H	$\rho = 7500\,\mathrm{kg/m^3}$, $c_{11} = c_{33} = 126$ GPa $c_{13} = 84.1$GPa, $e_{31} = -6.5\,\mathrm{C/m^2}$ $e_{33} = 23.3\,\mathrm{C/m^2}$, $d_{33} = 1.3 \times 10^{-8}\,\mathrm{F/m}$
ISD112	$\rho = 1600\,\mathrm{kg/m^3}$, $\nu = 0.5$ $E_o = 1.5$ MPa, $E_\infty = 69.95$ MPa $\alpha = 0.7915$, $\tau = 1.4052 \times 10^{-2}$ ms

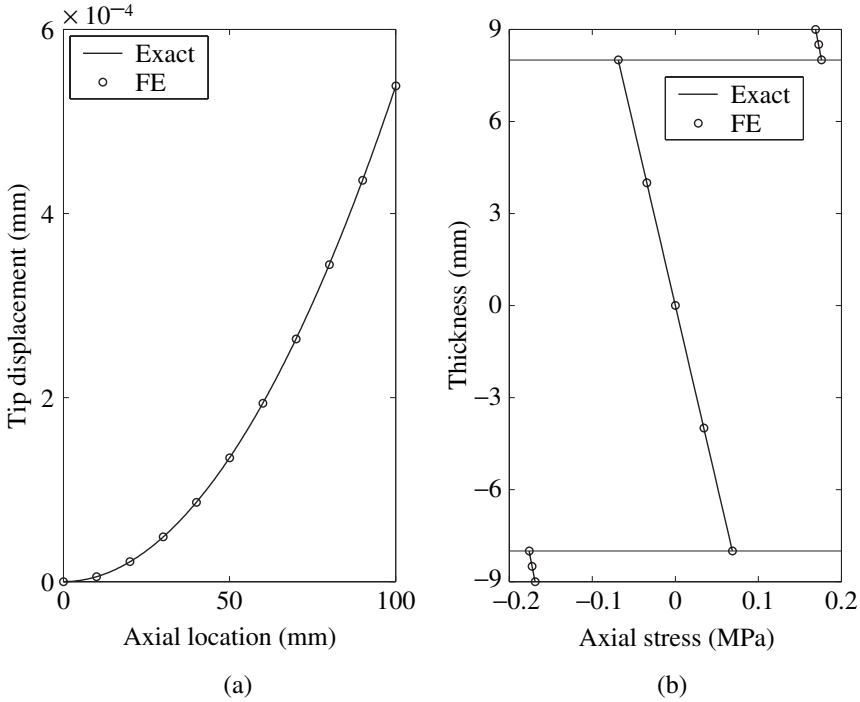

Figure 2. *(a) Tip displacement vs axial location and (b) axial stress distribution through the thickness.*

provided with thin piezoelectric faces (PZT5H). The mechanical properties are given in Table 1. The total length of the beam is $L = 280$ mm and total thickness is $h = 4.2$ mm (0.20 mm for the core, 1.5 mm for each elastic face, and 0.50 mm for each piezoelectric sublayer). The exact three-dimensional solution is based on a mixed state-space approach previously developed for the free-vibration analysis of laminated piezoelectric plates actuated by transverse shear mechanisms (Deü and Benjeddou, 2002). Its version for extension actuation in cylindrical bending is employed here.

First, only the exact three-dimensional solution is presented in order to clearly show the through-thickness profiles of the mechanical and electrical variables. In the following, these variables are normalized using the maximum absolute value of the axial displacement $u_{x\max}$ and piezoelectric material properties

$$U_x = \frac{1}{u_{x\max}} u_x, \qquad U_z = \frac{1}{u_{x\max}} u_z,$$
$$\Phi_z = \frac{e_{31}}{c_{13} u_{x\max}} \phi, \qquad D_z = \frac{L}{e_{31} u_{x\max}} D_3 \tag{44}$$

where U_x and U_z are the nondimensional axial and transverse displacements, and D_z and Φ_z are the nondimensional electric transverse displacement and potential.

The exact three-dimensional solution of the open-circuited simply supported sandwich beam for the first bending mode is shown in Figure 3. The evolution of the axial displacement through the thickness, computed at $x = 0$ or $x = L$, is plotted in Figure 3(a) with a thick solid line. One can observe in this figure the interest of working with a sandwich formulation since piezoelectric–elastic faces are much stiffer than the elastic core. In the same figure, the evolution of the transverse displacement at $x = L/2$ is presented (dashed line). Although the transverse displacement has a nonlinear shape, its value is quasi-constant (from approximately 75.4825 up to 75.4875 in the top scale). In Figure 3(b), the evolution of electric transverse displacement and potential through the thickness is plotted. Both are computed at $x = L/2$. Electric transverse displacement and potential distributions are strongly dependent on the electric boundary conditions and the mode type (Deü and Benjeddou, 2002). For the first bending mode and open circuit conditions, the electric transverse displacement is parabolic within the piezoelectric sublayer (dashed line). Under the same conditions, the electric potential in the piezoceramic face is slightly nonlinear (thick solid line).

Exact and numerical first nine natural frequencies of the sandwich beam with short- and open-circuited piezoelectric faces are presented in Table 2. Owing to the supplementary stiffness added to the system by means of the electromechanical coupling when the piezoelectric layers are treated as sensors, the natural frequencies are higher in the open-circuit case than in the closed-circuit one. It is noted that the error committed by the finite element approximation does not exceed 0.40%. In order to illustrate this good agreement between analytical and numerical solutions,

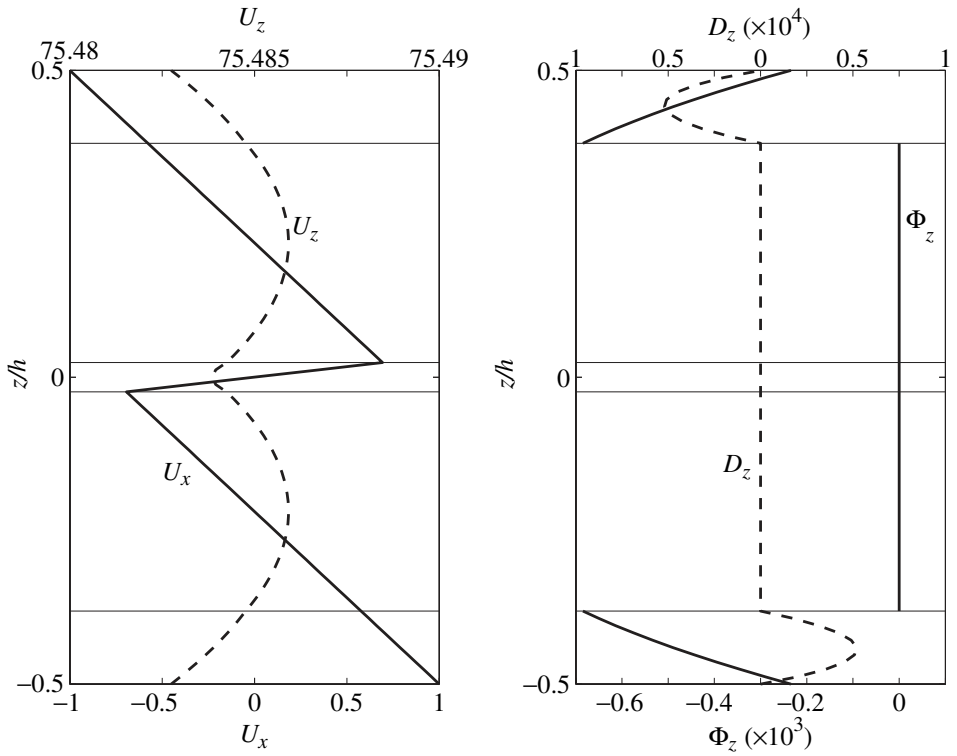

Figure 3. *Exact three-dimensional solution of the open-circuited simply supported sandwich beam for the first bending mode: (a) nondimensional axial (at x = 0 or x = L) and transverse (at x = L/2) displacement through-thickness distributions and (b) nondimensional electric transverse displacement (at x = L/2) and potential (at x = L/2) distributions.*

Table 2. First nine bending eigenfrequencies (Hz) of the sandwich beam with open- and short-circuited piezoelectric layers.

	Short circuit			Open circuit		
	Exact	Numerical	Error (%)	Exact	Numerical	Error (%)
1	65.492	65.375	0.178	70.803	70.697	0.150
2	219.687	219.166	0.237	237.552	237.088	0.195
3	469.881	468.784	0.234	508.546	507.614	0.183
4	818.493	816.848	0.201	886.208	884.937	0.143
5	1265.682	1263.785	0.150	1370.625	1369.464	0.085
6	1811.129	1809.613	0.084	1961.385	1961.188	0.010
7	2454.321	2454.225	0.004	2657.862	2659.974	0.079
8	3194.618	3197.455	0.089	3459.284	3465.621	0.183
9	4031.272	4039.096	0.194	4364.756	4377.881	0.301

Figure 4 presents the mechanical displacement field evolution through the thickness calculated for the first natural frequency when the piezoelectric layers are short and open circuited. In Figure 4(a), the axial displacement through-thickness distribution is shown. A very good agreement between the exact and the finite element solution is noted. In particular, a constant approximation for the transverse displacement is quite enough in this case (Figure 4(b)). Concerning the electric potential, due to the limitations on its approximation (see Equation (6)), one can only reproduce the voltage between the top and bottom surfaces of the piezoelectric faces. In order to compare this value with the exact one, one can extract from Figure 3(b) the difference of potential between the top and bottom surfaces of the piezoelectric sublayer. Hence, the absolute nondimensional value of the induced voltage measured within the piezoelectric layers for the finite element solution is 4.5048×10^{-4} and for the exact one is 4.5044×10^{-4}. As expected, in all the cases, the exact solution is very well approximated by the proposed finite element formulation.

RESULTS AND DISCUSSION

The present analysis consists of a cantilevered sandwich beam with a viscoelastic core (ISD112 at 27°C) constrained by symmetrical elastic faces (aluminum) with piezoelectric patches (PZT5H), as shown in Figure 5. The top piezoelectric patch works as an actuator and the bottom one as a sensor. The material properties and geometry data of the structure are shown in Table 1 and Figure 5, respectively. The beam is discretized by a regular mesh with 56 elements distributed as: two elements between the clamped end of the beam and the left edge of the piezoelectric patch, 14 along the patch, and 40 elsewhere. The mechanical excitation is performed by means of a transverse triangular impulse at the free end of the

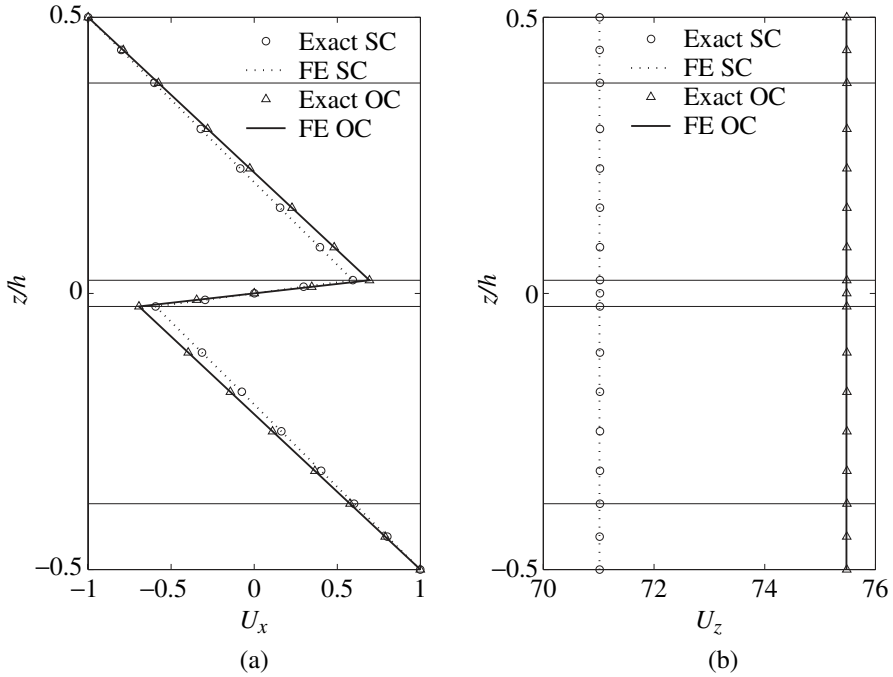

Figure 4. *Nondimensional (a) axial and (b) transverse displacement through-thickness distribution calculated for the first natural frequency when the piezoelectric layers are short- and open-circuited.*

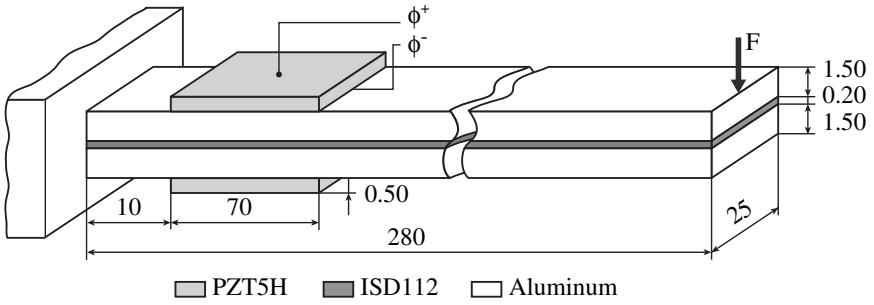

Figure 5. *Geometry data for the sandwich beam (in mm).*

beam, whose duration is 4 ms and amplitude 1 N. The study is performed up to 200 ms with a fixed time step $\Delta t = 1$ ms.

The validation of the implementation of the fractional derivative model is first focused. For this case, the top piezoelectric patch in Figure 5 is short-circuited. The crucial question is how to truncate the Grünwald series without losing information on the damping character of the viscoelastic material. Figure 6 shows the time evolution of the tip displacement for various values of truncation. When taking either 10 terms (dotted line) or the whole history, i.e., 200 terms (dashed line), dynamic responses of the beam are very close. However, if only five terms (solid line) are retained in the series, the amplitude of the transverse displacement is overestimated. In order to better understand such a behavior, the error (in total dissipated energy) versus the number of terms in the Grünwald expansion of the fractional operator approximation is plotted in Figure 7. This error is expressed by $(\|D_{\text{ref}} - D\|)/(\|D_{\text{ref}}\|)$, where D is related to the passive treatment only and given by $D = U_d - W_d$, with:

$$\left[U_d\right]_{t_n}^{t_{n+1}} = \frac{1}{2}(\mathbf{q}^{n+1} - \mathbf{q}^n)^T(\bar{\mathbf{F}}^{n+1} + \bar{\mathbf{F}}^n)$$

$$\left[W_d\right]_{t_n}^{t_{n+1}} = \frac{1}{2}(\mathbf{q}^{n+1} - \mathbf{q}^n)^T\bar{\mathbf{K}}(\mathbf{q}^{n+1} - \mathbf{q}^n)$$

where D_{ref} is the total dissipated energy associated to the reference solution. The so-called reference solution is computed with all the terms in the Grünwald series. Points A and B in Figure 7 are related to solid and dotted lines in Figure 6. It is noted that a noticeable error is committed when only five terms are taken to truncate the series ($\approx 2.52\%$), while for 10 terms this error considerably decreases ($\approx 0.16\%$). In fact, there is a constant time where the Grünwald series should be truncated (Galucio et al., 2004). For example, the point A corresponds to an underestimation of the fading memory phenomena, since five terms are not

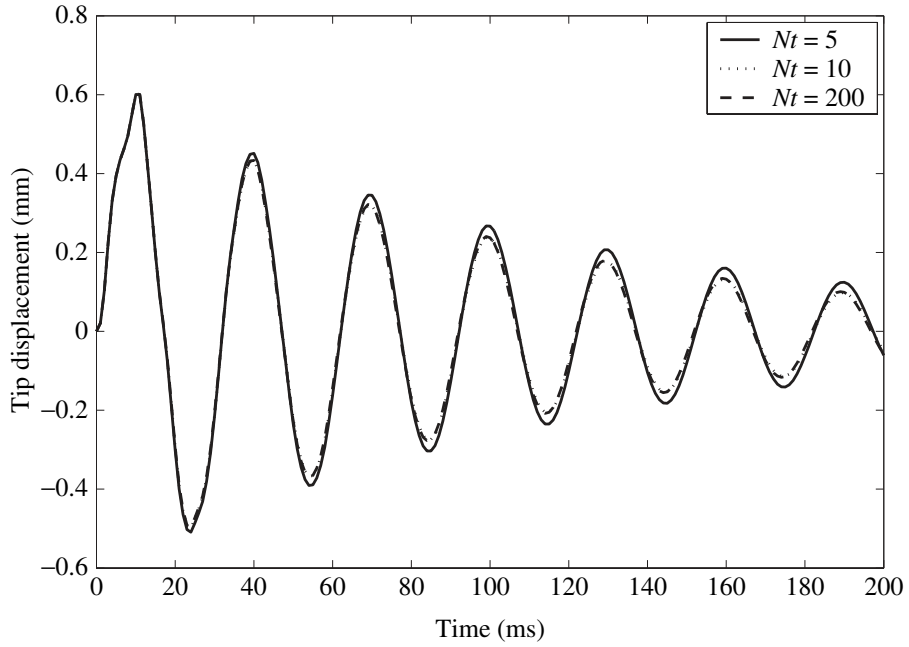

Figure 6. *Transverse tip displacement vs time for various values of N_t.*

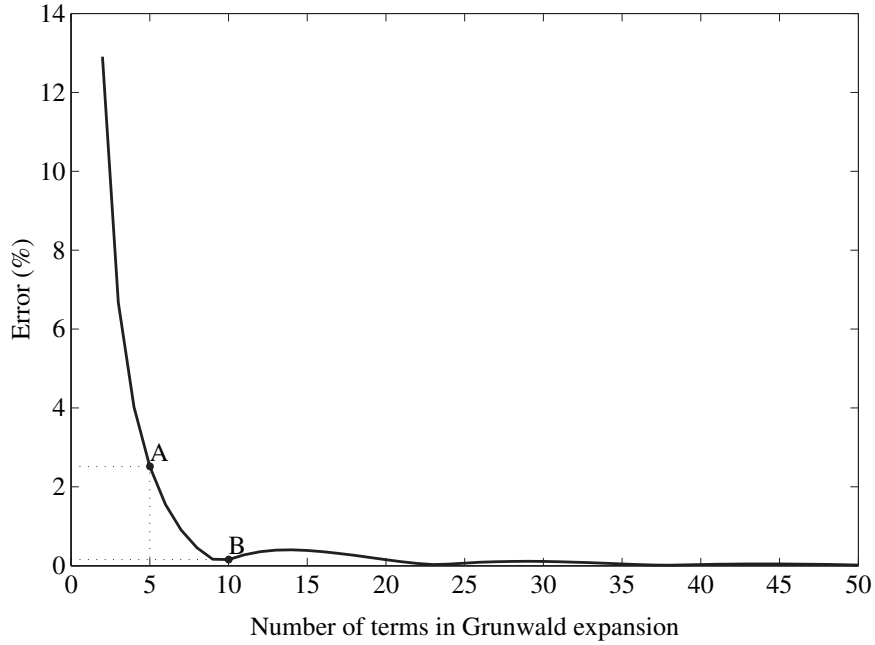

Figure 7. *Error in energy dissipation vs number of terms in the Grünwald expansion of the fractional operator approximation. Point A: $N_t = 5$ and Point B: $N_t = 10$.*

sufficient to accurately describe the viscoelastic behavior of the core.

The second part of this study is addressed to the hybrid piezoelectric–viscoelastic treatment for controlling vibrations arising from transient excitations. In the following example, both piezoelectric patches are activated and the fractional operator is approximated with the whole history in the Grünwald series. A sensor voltage feedback control scheme is used. The time derivative of the voltage measured in the sensor is used for the feedback signal and then applied to the top piezoelectric patch with a constant gain K_d, as $V_A = -K_d \dot{V}_S$. In Figure 8, the enhancement of the passive damping treatment (solid line) when a closed-loop control is applied for two constant gains -2 ms (dotted line) and -6 ms (dashed line) is observed. As expected, the results show that the combination of the active and passive damping treatments is more effective than the passive damping treatment only.

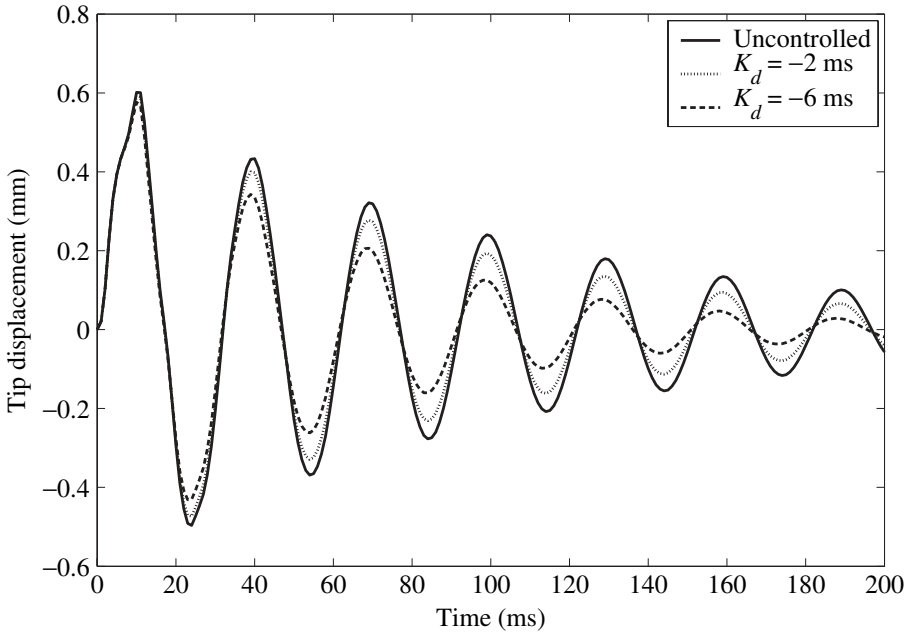

Figure 8. *Transverse tip displacement vs time for various values of K_d.*

CONCLUSION

A finite element formulation for transient dynamic analysis of sandwich beams with active constrained layer damping treatment is proposed. The sandwich beam is composed of a viscoelastic core, which is entirely covered by elastic faces that are provided with piezoelectric patches on their top and bottom surfaces. No electrical degrees of freedom are introduced in the finite element formulation. The electromechanical coupling is taken into account by means of an augmentation of the stiffness of the piezoelectric layers for a sensor configuration. A four-parameter fractional derivative model is used to describe the viscoelastic behavior of the core. Fractional operators are approximated by the Grünwald discretization, requiring the storage at each time step of the recent history only. The present formulation allows a relatively simple finite element implementation of hybrid piezoelectric–viscoelastic damping treatments for controlling vibrations, which is validated through results found in the literature. Preliminary results using a simple proportional derivative feedback control scheme are performed in order to show the effectiveness of the proposed numerical approach.

REFERENCES

Bagley, R.L. and Torvik, P.J. 1983. "Fractional Calculus – A Different Approach to the Analysis of Viscoelastically Damped Structures," *AIAA Journal*, 21:741–748.

Baz, A. 1997. "Boundary Control of Beams Using Active Constrained Layer Damping," *Journal of Vibration and Acoustics*, 119:166–172.

Benjeddou, A. and Deü J.-F. 2001. "Piezoelectric Transverse Shear Actuation and Sensing of Plates, Part 1: A Three-dimensional Mixed State Space Formulation," *Journal of Intelligent Material Systems and Structures*, 12:435–449.

Deü, J.-F. and Benjeddou, A. 2002. "Exact Free-vibration Analysis of Laminated Plates with Embedded Piezoelectric Transverse Shear Actuators or Sensors," In: *Proc. Fifth World Congress on Computational Mechanics*, Mang, H.A., Rammerstorfer, F.G. and Eberhardsteiner, J. Publishers, Vienna, Austria.

Galucio, A.C., Deü, J.-F. and Ohayon, R. 2004. "Finite Element Formulation of Viscoelastic Sandwich Beams using Fractional Derivative Operators," *Computational Mechanics*, 33:282–291.

Golla, D.F. and Hughes, P.C. 1985. "Dynamics of Viscoelastic Structures – A Time-domain, Finite Element Formulation," *Journal of Applied Mechanics*, 52:897–906.

Lesieutre, G.A. and Lee, U. 1996. "A Finite Element for Beams Having Segmented Active Constrained Layers with Frequency-dependent Viscoelastics," *Smart Materials and Structures*, 5:615–627.

Pritz, T. 1996. "Analysis of Four-parameter Fractional Derivative Model of Real Solid Materials," *Journal of Sound and Vibration*, 195:103–115.

Schmidt, A. and Gaul, L. 2001. "FE Implementation of Viscoelastic Constitutive Stress-strain Relations Involving Fractional Time Derivatives," In: *Proc. Constitutive Models for Rubbers II*, A.A. Balkema, Publishers, Tokyo, Japan, pp. 79–89.

Trindade, M.A., Benjeddou, A. and Ohayon, R. 2001. "Finite Element Modelling of Hybrid Active-passive Vibration Damping of Multilayer Piezoelectric Sandwich Beams – Part I: Formulation; Part II: System Analysis," *International Journal for Numerical Methods in Engineering*, 51:835–864.

Yi, S. and Sze, K.Y. 2000. "A Finite Element Formulation for Composite Laminates with Smart Constrained Layer Damping," *Advances in Engineering Software*, 31:529–537.

Zhang, X.D. and Sun, C.T. 1996. "Formulation of an Adaptive Sandwich Beam," *Smart Materials and Structures*, 5:814–823.